crystals

MDPI

Article

Effect of Molybdenum Concentration and Deposition Temperature on the Structure and Tribological Properties of the Diamond-Like Carbon Films

Hassan Zhairabany [1], Hesam Khaksar [2], Edgars Vanags [3] and Liutauras Marcinauskas [1,4,*]

[1] Department of Physics, Kaunas University of Technology, Studentų Str. 50, 51368 Kaunas, Lithuania; hassan.zhairabany@ktu.edu
[2] Marian Smoluchowski Institute of Physics, Jagiellonian University, ul. Lojasiewicza 11, 30-348 Krakow, Poland; hesam.khaksar@uj.edu.pl
[3] Institute of Solid State Physics, University of Latvia, Kengaraga Str. 8, LV1063 Riga, Latvia; edgars.vanags@cfi.lu.lv
[4] Plasma Processing Laboratory, Lithuanian Energy Institute, Breslaujos Str. 3, 44403 Kaunas, Lithuania
* Correspondence: liutauras.marcinauskas@ktu.lt

Abstract: Two series of non-hydrogenated diamond-like carbon (DLC) films and molybdenum doped diamond-like carbon (Mo-DLC) films were grown on the silicon substrate using direct current magnetron sputtering. The influence of molybdenum doping (between 6.3 and 11.9 at.% of Mo), as well as the deposited temperature (between 185 and 235 °C) on the surface morphology, elemental composition, bonding microstructure, friction force, and nanohardness of the films, were characterized by atomic force microscopy (AFM), energy dispersive X-ray spectroscopy (EDX), Raman spectroscopy, and a nanoindenter. It was found that the increase in the metal dopant concentration led to a higher metallicity and graphitization of the DLC films. The surface roughness and sp^3/sp^2 ratio were obtained as a function of the Mo concentration and formation temperature. The nanohardness of DLC films was improved by up to 75% with the addition of Mo. Meanwhile, the reduction in the deposition temperature decreased the nanohardness of the DLC films. The friction coefficient of the DLC films was slightly reduced with addition of the molybdenum.

Keywords: Mo-doped diamond-like carbon; microstructure; friction coefficient; nano-hardness; deposition temperature

Citation: Zhairabany, H.; Khaksar, H.; Vanags, E.; Marcinauskas, L. Effect of Molybdenum Concentration and Deposition Temperature on the Structure and Tribological Properties of the Diamond-Like Carbon Films. *Crystals* **2024**, *14*, 962. https://doi.org/10.3390/cryst14110962

Academic Editor: Nan Kang

Received: 30 September 2024
Revised: 25 October 2024
Accepted: 29 October 2024
Published: 5 November 2024

1. Introduction

Metal-doped diamond-like carbon films (Me-DLC) have been widely synthetized using dopants such as Ag, Ti, Cr, Cu, Ni, and Mo, and are becoming an ultimate choice to achieve preferred functionality and improve the micro-structure, adhesion, electrical, mechanical, and tribological properties of diamond-like carbon (DLC) films [1–6]. R.L. Leonard et al. [2] successfully proved that DLC films have the potential to enhance the performance of biomedical implants and instruments. M. Zhang et al. [3] found that the surface roughness of the Ti-DLC films with Ti interlayers slightly increased to 3.3 nm with the increase in the Ti content up to ~27 at.%; meanwhile, the hardness decreased to 8.9 GPa as the Ti content increased up to ~10 at.% due to the destruction of the carbon network before it increased up to 10.5 GPa at a high Ti content of ~27 at.% as more nanocrystalline carbides formed. J. Liu et al. [4] summarized the updated processes in recent years for modified DLC-coated rubber. They illustrated how the wear-resistant property of the rubber could be enhanced and where the surface could exhibit a low CoF of 0.2 with good adhesion between the DLC and the rubber surface after Ar plasma treatment. S. Gayathri et al. [5] investigated the effect of transition metal dopants on the tribology of the DLC films with 20 at. % of metal, and they found that the friction coefficient was lowest in Ag-DLC films compared with Ni-DLC and Ti-DLC films due to the high fraction of sp^2 and the

dispersion of soft Ag nanoparticles. Also, they indicated that the film/substrate adhesion was improved due to the decrease in the internal compressive stress of the films. L. Swiatek et al. [6] found that coating with a specific low amount of Si and Ag led to enhanced hardness, and they also found the best biocompatibility, suggesting that the Si/Ag-DLC film is a promising antibacterial biomaterial candidate for bio-medical applications.

Several researchers in the literature have proved the molybdenum dopant's role in improving tribological and mechanical properties, decreasing the compressive stress and friction coefficient, and improving hardness and biocompatibility [7–10]. Our previous study [7] indicated that the Mo dopant could be used to reduce the sp^3 site fraction, change the friction coefficient values, and improve the hardness of the DLC films. Y. Su et al. [8] verified that the Mo-DLC films synthesized at an appropriate bias voltage had stable friction coefficient values and low wear rates, with the highest nano-hardness values in the methanol ambient. M. Constantinou et al. [9] showed that the molybdenum doping could be used to enhance the nanoscratch resistance of DLC films. H. Sun et al. [10] reported that Mo with other carbide-forming elements like W, Ti, and Cr can break the sp^3 carbon bond or tetrahedral sites and initiate the graphitization of DLC films, which causes a decrease in the hardness and Young's modulus (which is not significant for low dopant contents).

The coating synthesis methods also have a key role in the final properties of metal-doped DLC films, especially the deposition temperature, where some applications such as high-speed cutting and aero engine bearing require a high temperature of 200 °C or more [11]. At this condition, the wear becomes intense, and liquid lubricants cannot protect the surfaces properly due to the oxidation and decomposition. Thus, solid-lubricating films such as coating materials become an unavoidable choice if the original mechanical properties of the substrate are excellent, and it is required to be preserved [12]. Several researchers have tried to explore and interpret the influence of the deposition temperature on the structure and properties of DLC films [13–16]. Q. Zeng and Z. Ning [13] found that the DLC films demonstrated low friction coefficients due to graphitization and dehydrogenation at a 400 °C temperature. Moreover, the addition of dopants such as chromium, titanium, and other elements improved the failure temperature of DLC films up to 800 °C. R. K. Ghadai et al. [14] studied the temperature influence on the mechanical properties of Ag-DLC coatings, and the authors found that the films' hardness and Young's modulus were reduced with the increase in the deposition temperature. The residual stress was also significantly low at 950 °C. Y. Chen et al. [15] indicated that the addition of molybdenum-desulphated enhanced the adhesion and reduced the internal stress of MoS_2-DLC films; however, doped DLC films demonstrated lower hardness and elastic modulus values. Additionally, the coating with a specific dopant content achieved brilliant anti-friction and anti-wear behavior in the temperature range of 25–450 °C. B. Huang et al. [16] observed that the sp^3/sp^2 ratio values and the hardness of the Si-DLC coatings increased first before decreasing as the deposition temperature increased from 60 °C to 180 °C. It was indicated that the Si-DLC film obtained at 120 °C revealed the lowest wear rate and friction coefficient and had the highest hardness and sp^3 bond fraction. Meanwhile, information on the influence of the substrate temperature on the structure and properties of Mo-DLC films is still lacking.

In this work, the DLC and Mo-doped DLC thin films were deposited by a direct current (DC) magnetron sputtering technique. The aim of the work was to investigate the influence of the synthesis temperature (distance) on the microstructure, elemental composition, hardness, and tribological properties of DLC and Mo-DLC films. It should be highlighted that the effect of the deposition temperature has been rarely investigated in the literature or in our previous study [7] for Mo-doped DLC films, nor has the relation between the deposition temperature and the deposition distance.

2. Materials and Methods

DLC films and Mo-doped DLC films (Mo-DLC) were produced by means of DC magnetron sputtering deposition. Graphite (carbon) and molybdenum magnetron targets with

a 76.2 mm diameter and 6 mm thickness were used. Graphite (99.9%, Kurt J. Lesker Company, Saint Leonards, UK) and molybdenum (99.95% purity, Testbourne Ltd., Helmond, The Netherlands) disc targets were used. The targets–substrate distances were adjusted at 4 cm, 6 cm, and 8 cm in order to obtain different deposition temperatures. The temperature was measured using a thermocouple fixed on the silicon sample holder. The maximum temperature of each film was reached after 7 min of deposition (Table 1). The DLC and Mo-DLC films were deposited on silicon (100) substrates. The films were deposited at 4, 6, and 8 cm distances from the targets, and the Mo amount was controlled by using a slit opening of about 28 mm on a shield mounted above the molybdenum target [7,17].

Table 1. Synthesis conditions and atomic composition of the deposited films.

Samples	Target-Substrate Distance [cm]	Slit Opening [mm]	Temperature [°C]	Carbon [at.%]	Oxygen [at.%]	Molybdenum [at.%]
DLC1	4	---	235	92.5 ± 1.0	7.5 ± 0.3	---
DLC2	6	---	210	93.4 ± 2.3	6.6 ± 1.2	---
DLC3	8	---	185	91.2 ± 2.1	8.8 ± 1.3	---
Mo-DLC1	4	28	235	79.9 ± 1.3	8.2 ± 0.6	11.9 ± 0.3
Mo-DLC2	6	28	220	80.2 ± 0.5	11.3 ± 1.0	8.5 ± 0.2
Mo-DLC3	8	28	185	79.6 ± 1.3	14.1 ± 0.7	6.3 ± 0.17

The elemental composition of the carbon films was determined by energy dispersive X-ray spectroscopy (EDX) (Bruker Quad 5040 spectrometer, Germany, Hamburg). The measurements were performed on 3 different points using 10 kV. The bonding structures of the as-deposited DLC and Mo-DLC films were determined by Raman spectroscopy (Renishaw, Wottonunder-Edge, UK) with a CCD camera equipped and confocal microscope (50× objective), and a semiconductor laser with 532 nm wavelength was used. The Raman spectra were recorded using 2400 lines/mm grating, the exposure time was set to 10 s, the amount of accumulations was 10, the laser power was 0.3 mW, and the laser spot diameter was ~10 µm. The Raman spectra were recorded in 100–2000 cm^{-1} range on 3 different spots for each as-deposited film. The Gaussian function was used to fit Raman spectra of films using two peaks in the 1000–1800 cm^{-1} range. Nanoindentation tests were performed with an MTS-Agilent G200 nanoindenter (MTS Systems, Eden Prairie, MN, USA), employing the continuous stiffness measurement (CSM) technique for thin films. Calibration of the Berkovitch diamond tip's area function was performed with fused silica as the reference material. The indentation depth was set to 1000 nm. Thermal drift during the tests was compensated using the instrument's drift correction feature. The testing parameters were as follows: target strain rate of 0.05 s^{-1}, target harmonic displacement of 2 nm, and a frequency target of 45 Hz. The substrate's Young's modulus was set at 152 GPa, with a Poisson's ratio of 0.27 for the substrate and 0.20 for the film (default). For each DLC or Mo-DLC film, approximately 18 to 27 indentations were carried out in a 9 × 9 array, where the distance between indents was 30 microns. Faulty data points were identified and removed before calculating the average hardness and Young's modulus values of the films. The atomic force microscopy (AFM) measurements were carried out using DriveAFM (Nanosurf, Liestal, Switzerland) to determine the surface morphology, where the measurements were made on 3 spots of each sample with an area of (10 × 10) μm^2. The surface roughness values (such as R_a, RMS, skewness, and kurtosis) were calculated as the average values obtained from these three measured areas. These values can be obtained from Gwyddion software [18] using the statistical analysis tools; more information can be found here [19]. The friction coefficient of the thin films was obtained using the same AFM with a PPP-LFMR-10 AFM probe (Nanosensors™, Neuchatel, Switzerland), with a nominal tip radius of less than 7 nm and a measured spring constant of about 30 N/m [20,21]. The measurements were performed in the air at room temperature with lateral force mode on 3 different spots of each film with an area of 10 × 10 µm, and the applied loading was progressive from 10 nN to 45 nN. After measuring the friction, the values were calibrated following the

methodology presented in [22]. The detailed technical data regarding the determination of friction coefficient can be found in our previous study [7].

3. Results and Discussion

3.1. Elemental Composition Analysis

The elemental composition values of the coatings are given in Table 1. These values were calculated as the average of three different spots, and the error was determined as the standard deviation. The thickness of the deposited films varied from 150 to 200 nm; thus, the EDX measurements indicated a significant concentration of silicon (due to Si substrate) compared to elements obtained in the coating, like carbon, oxygen, and molybdenum. Contemplating that these measurements aimed to investigate the elemental composition of the films and of the substrates, the atomic percentage was normalized, excluding the silicon element.

The concentrations of carbon and oxygen slightly changed between 91.2 and 93.4 at.% and 6.6 and 8.8 at.%, and the deposition distance varied between 4 and 8 cm for amorphous carbon films. The EDX results indicated that the Mo content was ~11.9 at.% when the deposition was performed at the highest substrate temperature (Table 1). Meanwhile, the content of the Mo was 8.5 at.% in the Mo-DLC films, which was obtained when the synthesis was performed at a 6 cm distance. The further increase in distance (reduction in substrate temperature) reduced the Mo concentration in the film to 6.3 at.%. It should be noted that the increase in the target–substrate distance led to an increase in the oxygen content from 8.2 to 14.1 at.%. As the deposition was performed at 2-3 Pa of argon plasma, a small amount of the residual air could be found in the vacuum chamber. The increase in the oxygen content in the Mo-DLC with the reduction in the temperature (increase in the distance) was due to entrapment of the residual air in the argon plasma. As the distance was increased, it took longer for the atoms to reach the substrate. Thus, the probability of carbon or/and molybdenum atoms sputtered from the targets to interact with the oxygen was higher. This resulted in an increase in the amount of carbon–oxygen and molybdenum–oxygen sites in the films. Additionally, the kinetic energy of the Mo or C atoms arriving at the substrate at longer distances (lower temperature) was lower, and this could also contribute to the production of more oxygen bonds in the metal-doped DLC films [8,23]. The amount of metals in the DLC films also affected the oxygen concentration. It was determined that the oxygen content increased from the 5.7 to 20.5 at.% with the enhancement in the W content from 2.6 to 34.5 at.% in the Ti/W-DLC films [23]. Also, the increase in the Ti content in the DLC films could lead to a higher oxidation of the films after the deposition process [3]. It is well known that molybdenum atoms can bond with carbon and oxygen to create carbides and oxides. As the temperature or Mo concentration decreased, the content of the molybdenum carbides in the Mo-DLC films was lower [8,23]. Therefore, it was likely that as the temperature decreased, more and more molybdenum atoms would bind to oxygen, and as a result, the oxygen concentration in the films was higher compared to Mo-DLC coatings obtained at higher temperatures.

3.2. Surface Morphology

The surface morphology and roughness are crucial factors in examining the tribological behavior of DLC films. Thus, the surface morphology of the films was measured by AFM, as presented in Figure 1. All synthesized films had smooth surfaces, with randomly distributed large size grains. The highest number of large grains was detected for the DLC3 film. The surface roughness data demonstrated that the introduction of the Mo dopants led to the formation of Mo-DLC films with smoother surfaces.

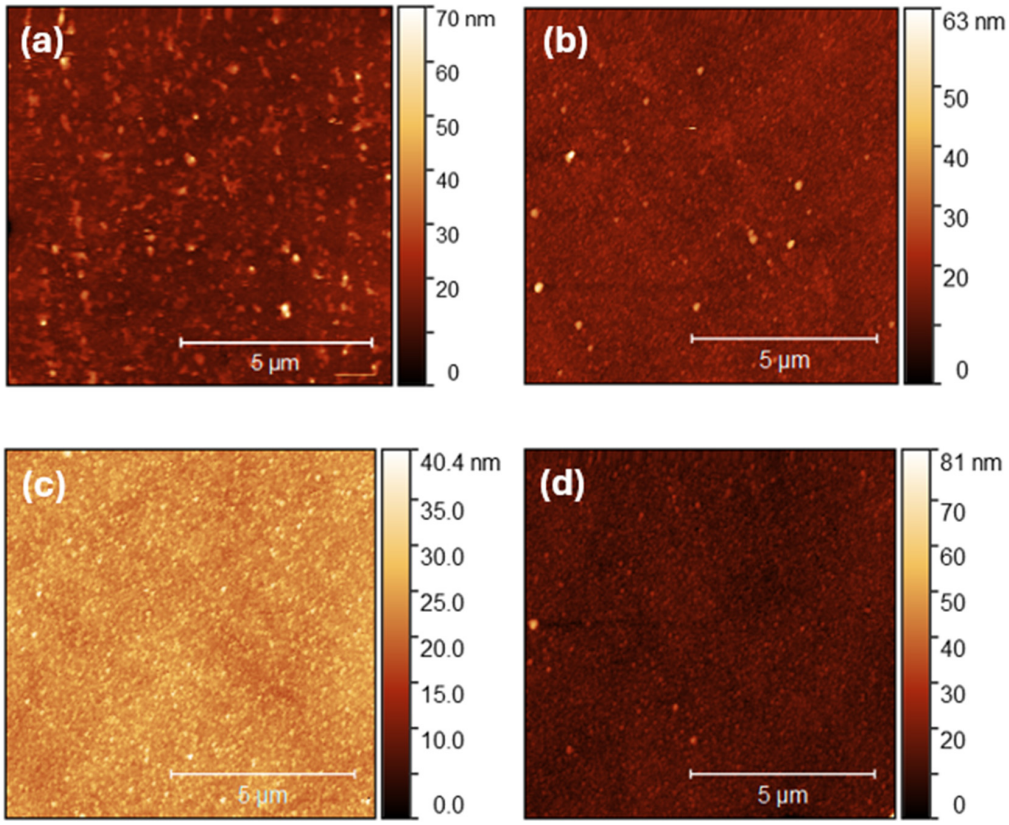

Figure 1. Surface morphology of the films: (**a**) DLC3, (**b**) Mo-DLC1, (**c**) Mo-DLC2, and (**d**) Mo-DLC3.

The variation in the average surface roughness (R_a) and the root mean square (RMS) surface roughness with the substrate–target distance of the undoped DLC and the Mo-doped DLC films are given in Figure 2. It is well known that the surface roughness values are affected by the thickness of the films, as the formed DLC and Mo-DLC films should have similar thickness of about 200 nm, as obtained in our previous research [7]. Thus, the influence of the thickness on the surface roughness values of these films was probably insignificant. The surface roughness values of DLC films slightly increased with the increase in the substrate–target distance, as shown in Figure 2.

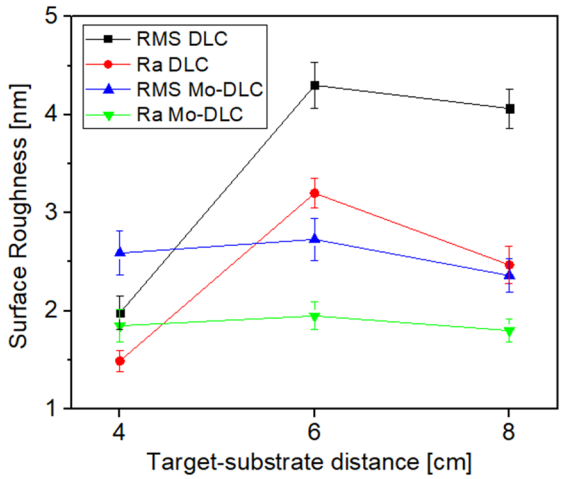

Figure 2. Surface roughness versus target–substrate distance and Mo content.

The R_a and RMS roughness values of the DLC1 films were 1.5 and 2.0 nm, respectively. The further increase in the distance more than twice increased the R_a and RMS values of the DLC2 film by up to 3.2 and 4.3 nm, respectively. The DLC film deposited at the lowest

temperature demonstrated a slight reduction in the R_a and RMS values down to 2.5 nm and 4.0 nm, respectively. Meanwhile, the variation in the substrate temperature had no effect on the R_a and RMS values of Mo-DLC films, which were almost stable given values of 1.9 and 2.6 nm, respectively. The skewness and kurtosis values for the DLC1, DLC2, and DLC3 films were 0.9 and 2.5, 1.1 and 2.9, and 1.3 and 2.4, respectively. Meanwhile the skewness and kurtosis of the Mo-DLC1, Mo-DLC2, and Mo-DLC3 films were 3.2 and 5.0, 3.1 and 4.8, and 0.6 and 7.1, respectively. These results demonstrate that the addition of Mo enhanced the skewness and kurtosis of the DLC films. As these values are close to zero, this indicates that the surface morphology is mostly uniform and does not exhibit heavy deviations from surface height. The increase in the kurtosis values for Mo-DLC films could be due to the presence of some randomly distributed uneven local features on the surfaces [24].

It has been reported in the literature that the DLC films have RMS values of about 1 nm or less, as shown by R. L. Leonard et al. [2], M. Zhang et al. [8], and others [9–13]. Y. Su et al. [8] deposited a series of Mo-DLC films onto silicon substrates, where the Mo content was almost stable at around 7 at.% for all samples, and the average surface roughness was between 1 nm and 2 nm for the samples with low oxygen contents of between 4.0 to 5.4 at.%. It was observed that the surface roughness value increased up to 3.45 nm for the DLC film with a higher oxygen content of 9.3 at.%. A similar work was conducted by M. Constantinou et al. [9], where the RMS values slightly increased from 0.11 to 0.25 nm with Mo doping up 3.2 at.%. Other metals, like titanium, showed close values and trends; it was reported by M. Zhang et al. [3] that the RMS values gradually increased from 1.57 to 3.32 nm with the increase in the Ti content up to 27 at.%. It was found that the R_a values of the Ag-DLC films increased with the increase in temperature. The lowest and the highest R_a values were 4.8 and 71.2 nm for the Ag-DLC films formed at temperatures of 800 and 950 °C, respectively [12]. These results indicate that the increase in metal dopant content led to a higher metallicity of the coating and increased the surface roughness. Another reason for the increase in surface roughness could have been the graphitization of the DLC films due to doping with molybdenum, in which the amount of sp^2 C=C bonds increased and the fraction of sp^3 C-C sites decreased.

3.3. Raman Spectroscopy Data

The Raman spectra analysis focused on the region between 1000 and 1800 cm^{-1}, since the peaks assigned from the A_{1g} breathing (D-band) of disordered sp^2 carbon atoms sites such as the aromatic ring structure and E_{2g} stretching mode (G-band) of the disordered sp^2 of all pairs of aromatic and olefinic molecules were dominated [25]. The Raman spectra of the DLC and Mo-DLC films are given in Figure 3a–d. Figure 3a,b show the normalized Raman spectra of DLC and Mo-DLC films, and the difference in the spectra intensity can be noticed. Figure 3e–g illustrates the variation in the main Raman spectra parameters, such as G peak positions, intensity ratios of the D peak to the G peak (I_D/I_G), and the full width at half maximum of the G band ($FWHM_G$) of the films versus the deposition temperature (distance). The increase in the substrate–target distance from 4 to 8 cm decreased the temperature from 235 to 185 °C. However, the reduction in the temperature had no effect on the G peak positions for the DLC and Mo-DLC films (Figure 3e). The G peak positions were about ~1577 cm^{-1} and ~1573 cm^{-1} for the DLC and Mo-DLC films, respectively. The I_D/I_G ratio for the DLC films was reduced from 0.96 to 0.85 with the reduction in the deposition temperature.

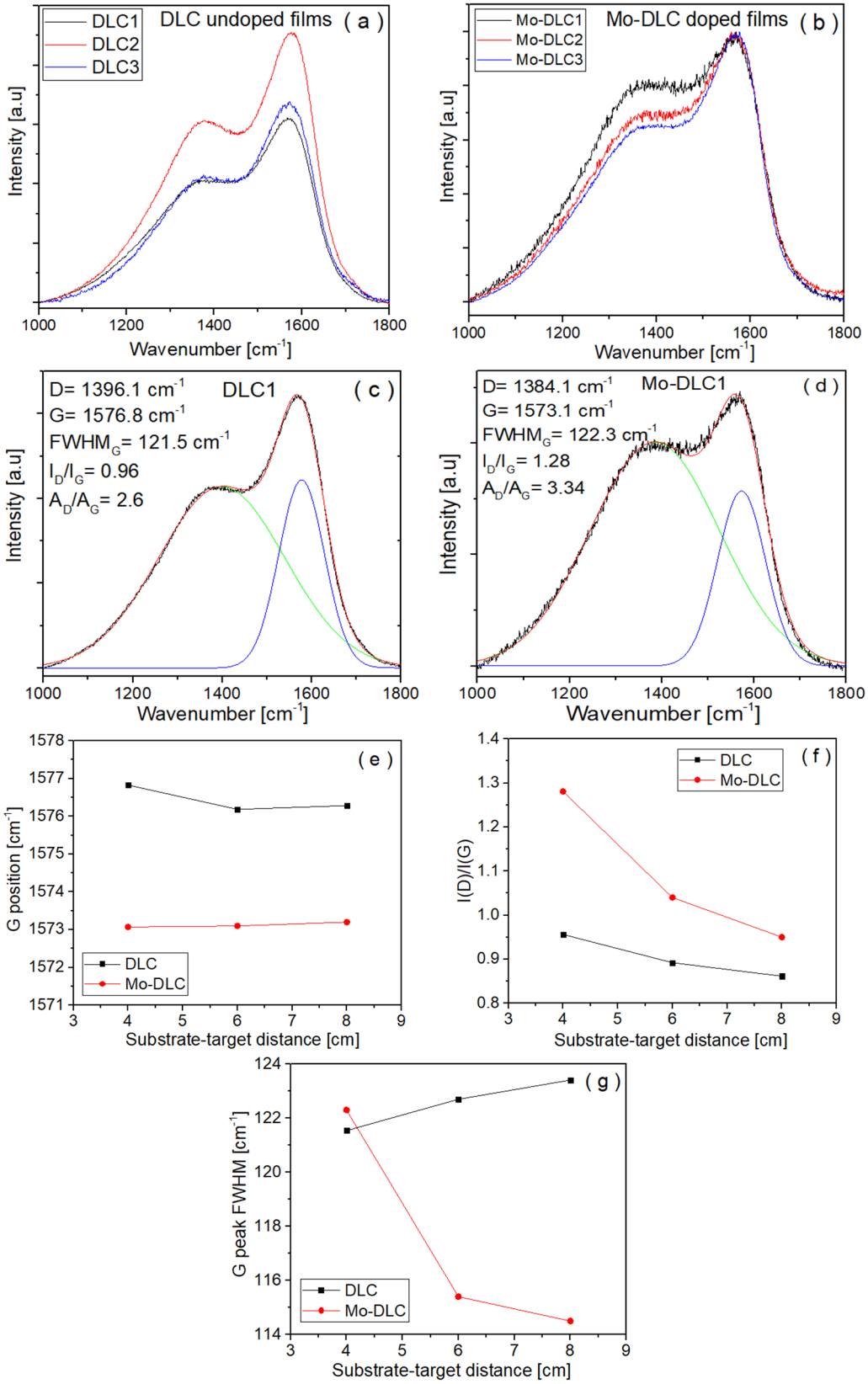

Figure 3. Raman spectra of the DLC (**a**), Mo-DLC (**b**), DLC1 (**c**), and Mo-DLC1 (**d**) films; variation in the characteristic parameters of films versus the substrate–target distance (**e**–**g**).

A similar trend was observed for the Mo-DLC films. The I_D/I_G ratio value dropped from 1.28 to 0.96 with the decrease in the temperature (Figure 3f). However, the $FWHM_G$

values of the DLC films slightly widened from 121.5 to 123.5 cm^{-1}, while the $FWHM_G$ values of the Mo-DLC films were reduced from 122.3 to 114.5 cm^{-1} with the increase in the distance (Figure 3g). V. S. Yadav et al. [25] found that, at a higher substrate temperature, the sp^3 contents were higher (for DLC between 100 and 300 °C). Also, this was due to an increase in the size of the sp^2 nanoclusters in the carbon matrix of the films. It was also reported that the increase in the I_D/I_G ratio of the metal-doped DLC films or DLC films was associated with a lower sp^3 carbon bond fraction, and this is also an indication of an increase in the size of the sp^2 cluster in the films [26,27]. This could explain the trend presented in Figure 3f, where the I_D/I_G ratio of the films was reduced with the decrease in temperature. Reducing the I_D/I_G ratio demonstrated a lower intensity of the D peak associated with the reduction in the content of aromatic disorder rings and a higher sp^3 C–C content [17,27]. The reduction in the temperature allowed for the deposition of the DLC films with a higher sp^3 bond content. The temperature effect can be seen between the Mo-DLC3 film deposited at a lower temperature of 185 °C and the Mo-DLC1 film formed at higher temperature of 235 °C, where the increase in the I_D/I_G and $FWHM_G$ with the decrease in the G peak position was reported by V. S. Yadav et al. [25]. The trends of these parameters were due to promotion of the sp^2 cluster in the coating with a higher temperature. Additionally, the higher I_D/I_G ratio and narrower $FWHM_G$ values of the Mo-DLC films signaled an increase in the sp^2 carbon sites in the films. It should be noted that the increase in the oxygen concentration in the DLC films promoted the formation of sp^2 bonds and enhanced the size of graphitic clusters [17]. The Raman spectra results led to the suggestion that the addition of the Mo reduced the sp^3/sp^2 carbon site ratio in the DLC films. H. Li et al. [28] observed the enhancement in the sp^2 content and the formation of a larger size sp^2 cluster in the a-C films with the increase in the deposition temperature from 30 °C to 400 °C.

3.4. Determination of Friction Coefficient

The dependence of the friction force on the applied loads in the range from 10 nN to 45 nN on the surface of the DLC and Mo-DLC films was performed and is presented in Figure 4. The results demonstrated that the friction force was enhanced linearly with the increase in the normal force for the DLC and Mo-DLC films (Figure 4). For the DLC2 film deposited at 210 °C, the friction force proportionally increased from 2.4 to 5.8 nN with the increase in the applied load from 10 to 45 nN.

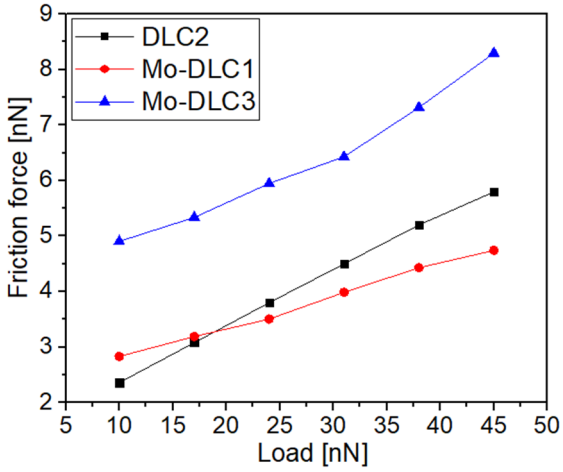

Figure 4. Dependence of nano-friction force versus applied load for the DLC and Mo-DLC films.

The determined coefficient of friction of the DLC2 film was ~0.1. The increase in the applied load from 10 to 45 nN enhanced the friction force of the Mo-DLC1 film from 2.8 to 4.7 nN (Figure 4). As a result, the lowest friction coefficient of ~0.056 was obtained. The friction force of the Mo-DLC3, deposited at the lowest temperature of 185 °C, rose

from 4.9 to 8.3 nN, which led to a friction coefficient of ~0.097. The results show that the friction coefficient was slightly reduced with a molybdenum doping, and likewise with the increase in the deposition temperature. A similar trend was observed by M. Constantinou et al. [9], where the CoF of the undoped DLC film was ~0.12 when the CoF was slightly reduced with addition of a low amount of Mo. However, the further increase in the Mo concentration up to 3.2 at.% slightly enhanced the CoF to ~0.13. The authors attributed this behavior to the higher roughness of the Mo-DLC films and to the increased shear resistance probably caused by the formation of Mo-C bonds in the carbon matrix [9].

In addition, Y. Chen et al. [15] found that the CoF of MoS_2-DLC composite films tested at 25 °C varied between 0.06 and 0.08 for the films with low amounts of Mo and S up to 4.4 and 4.7 at.%, respectively, while it increased to 1.3 with higher amounts of Mo and S, with 6.15 and 5.82 at.%, respectively. B. Huang et al. [16] tested the friction behavior of Si-DLC coatings at different deposition temperatures from 60 to 180 °C. For films deposited onto a stainless steel (316L) substrate, they observed a decrease in the CoF value from 0.18 to 0.03 in the deposition temperature range between 60 and 120 °C; then, there was a slight increase up to 0.08 at a temperature of 180 °C. The authors attributed this trend to the fact that the graphite content increased when the deposition temperature rose from 120 to 180 °C; this could explain why the Mo-DLC3 films had higher CoF values compared to Mo-DLC1 in our results (Figure 4). Moreover, it was concluded by Y. Wang et al. [29] that the presence of oxygen molecules led to a significant decrease in the friction force of DLC films. Although the oxygen content in the Mo-DLC3 was about 14.1 at.%, which is higher than that of Mo-DLC1 with 8.2 at.%, the Mo-DLC3 still had the higher CoF value. This shows the deposition temperature's influence compared to that of the oxygen content. In addition, Tomala et al. [30] obtained a decrease in the friction coefficient with the increase in the DLC film's graphitization, which agreed with the results herein, where the sp^2/sp^3 ratio increased with the increase in the synthesis temperature of Mo-DLC films.

3.5. Mechanical Properties Analysis

The variation in nano-hardness and Young's modulus versus the indenter penetration depth for the DLC and Mo-DLC films is illustrated in Figure 5. Table 2 contains the hardness and Young's modulus parameters of the films. These values were calculated up to 100 nm as the influence of the substrate began to take place after the half thickness of the coatings was estimated be up to ~200 nm. The results show that the hardness and Young's modulus were enhanced with Mo doping; the hardness increased from 3.86 to 6.76 GPa at a low temperature of 185 °C and from 8.03 to 10.99 GPa at a high temperature of 235 °C (Figure 5a,c). Also, the increase in the temperature led to an increase in the hardness and Young's modulus for both DLC and Mo-DLC films. The DLC film's nanohardness was increased from 3.86 to 8.03 GPa, and that of the Mo-DLC films from 6.76 to 10.99 GPa. It should be noted that the typical hydrogen-free a-C films have a higher hardness value than was obtained in our research [7]. The lower hardness value could be attributed to two reasons: one is the high fraction of sp^2 sites in the films, and secondly, a high amount of oxygen existed in the films. The increase in oxygen content led to a reduction in the hardness due to a higher fraction of C–O and C=O bond formation [31,32]. This second reason can explain the reduction in hardness values obtained for Mo-DLC1 and Mo-DLC2, where the deposition temperature was very similar, but the amount of oxygen in the Mo-DLC2 film was higher compared to the oxygen value determined in the Mo-DLC1 film.

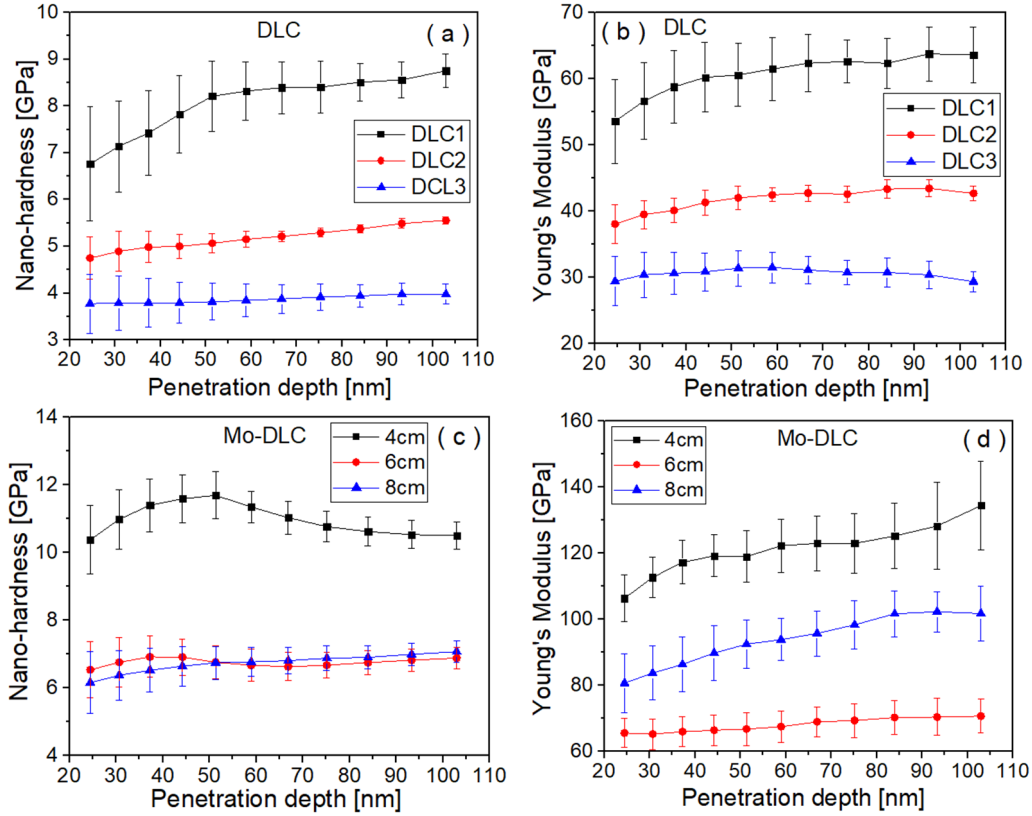

Figure 5. Nanohardness (**a**,**c**) and Young's modulus (**b**,**d**) of the DLC (**a**,**b**) and Mo-DLC (**c**,**d**) films.

Table 2. Hardness and Young's modulus of the deposited films.

Samples	Hardness (H) [GPa]	Young's Modulus (E) [GPa]	H/E	H^3/E^2 [GPa]	H^2/E [GPa]
DLC1	8.03 ± 0.65	60.56 ± 3.13	0.133 ± 0.004	0.141 ± 0.020	1.064 ± 0.119
DLC2	5.16 ± 0.25	41.68 ± 1.73	0.124 ± 0.003	0.079 ± 0.007	0.639 ± 0.041
DLC3	3.86 ± 0.08	30.60 ± 0.69	0.126 ± 0.004	0.062 ± 0.005	0.488 ± 0.025
Mo-DLC1	10.99 ± 0.46	120.99 ± 7.52	0.091 ± 0.007	0.091 ± 0.017	0.998 ± 0.110
Mo-DLC2	6.72 ± 0.27	93.34 ± 7.53	0.072 ± 0.003	0.035 ± 0.002	0.483 ± 0.009
Mo-DLC3	6.76 ± 0.12	67.93 ± 2.07	0.099 ± 0.003	0.067 ± 0.005	0.672 ± 0.031

Moreover, the results of Tang et al. [26] and Zhao et al. [33] show that the Mo adatoms and the created nanoparticles both disrupted the homogeneity of the carbon network, leading to a decrease in the hardness and elastic modulus. Meanwhile, other studies, such as Y. Su et al. [8], have found that the Mo doping improved the hardness of DLC film, as a hard MoC phase was formed in the coating. The highest nano-hardness of 16.0 GPa was obtained for the Mo-DLC film with a Mo content of 7.79 at.% and with a low amount of oxygen, ~4.21 at.%, due to the formation of the highest fraction of a hard MoC phase in this film. The introduction of Mo atoms led to the destruction of C-C cross-linked bonds, while the increase in the oxygen content led to the formation of low-hardness bonds, such as C-O and C=O bonds [34]. Thus, it could be one of the reasons for the decreased Mo-DLC film hardness when the deposition distance was enhanced. It should be noted that the hardness values of the films depended on the combination of the sp^3 bond fraction, the MoC phase amount, and the concentration of the oxygen in the films.

The mean hardness and Young's modulus values of the deposited DLC and Mo-DLC films, as well as the hardness/elastic (H/E, H^2/E, and H^3/E^2) ratios observed up to a depth of 100 nm, are given in Table 2. Tripathi et al. [35] determined that the H/E

ratio was attributed to wear resistance and elastic strain failure, and it varied between 0 (plastic behavior) and 0.1 (elastic behavior) for carbon coatings. The H^3/E^2 ratio was related to the plastic deformations, as it showed the ability of DLC films to absorb the load energy [35,36]. The results indicated that the H/E ratio of the DLC films was reduced from 0.133 to 0.126 with the decreases in temperature. Meanwhile, the H^3/E^2 ratio was reduced by more than two times from 0.141 GPa to 0.062 GPa when the temperature was reduced from 235 to 180 °C, respectively. The H/E ratio of the Mo-DLC films varied from 0.072 to 0.099. Meantime, the H^3/E^2 ratio varied from 0.035 to 0.091 GPa (Table 2). The addition of metals usually increases the plasticity of DLC films [3,8]. The addition of Mo reduced the intrinsic brittleness of the DLC films by allowing for more plastic deformation as metal clusters or molybdenum carbides were formed [8,9,26]. Thus, the elastic modulus values were improved, leading to lower H^3/E^2 ratio values of the Mo-DLC films. Also, the formation of the metal carbides at a higher metal concentration could effectively recover the disarrangement of the carbon network and reduce the sp^3 bond fraction in the metal-doped DLC films, thus leading to an increase in the hardness [3,8]. Usually, the higher the H/E and H^3/E^2 ratios, the better the toughness of the DLC film [16]. Thus, these results clearly show that the toughness of the Mo-doped DLC films was decreased with the addition of Mo dopant, showing the highest H/E, and the H^3/E^2 ratios stood for the DLC1 coating with 0.141 and 1.064 GPa, respectively. Meanwhile, the highest H/E, and H^3/E^2 ratio values for the Mo-doped DLC film were obtained when the deposition temperature was the highest, and these values were 0.091 and 0.998 GPa, respectively. The decrease in the substrate temperature promoted the formation of the sp^3 carbon sites, but also increased the fraction of carbon oxygen or molybdenum oxygen bonds. It is likely that, although the number of sp^3 bonds increased, this increase could not compensate for the increase in oxygen bonds, which was responsible for the reduction in the hardness of the DLC films. The obtained results demonstrate that the addition of the Mo allowed the sp^2/sp^3 bond ratio, friction coefficient, nanohardness, and elastic modulus of the DLC films to be controlled.

4. Conclusions

The DLC and Mo-DLC films were sputtered on a silicon substrate using direct-current magnetron sputtering. The concentration of molybdenum varied from 6.3 to 11.9 at.% depending on the temperature of deposition. The oxygen concentration in the films depended on the Mo concentration and synthesis temperature. The highest oxygen concentrations were observed in the DLC and Mo-DLC films deposited at the lowest temperature and were 8.8 at.% and 14.1 at.%, respectively. The surface roughness of the DLC films decreased with the addition of Mo dopants in the films and almost did not depend on the temperature of the deposition. Raman spectroscopy results indicated that the sp^2/sp^3 ratio increased and a slight graphitization of the films was promoted with the addition of Mo into the DLC films. Additionally, the increase in the deposition temperature promoted the growth of the sp^2 cluster in the coatings. The Mo dopants improved the nano-hardness and Young's modulus of the DLC films by up to 70%. The highest values of hardness (~11 GPa) and elastic modulus (~121 GPa) were observed at the 235 °C temperature of deposition for the Mo-DLC1 film. The highest friction coefficient of ~0.1 was obtained for the DLC2 film. The incorporation of Mo slightly reduced the friction coefficient of the doped DLC films. The lowest friction coefficient (~0.056) was observed for the Mo-DLC1 film deposited at a temperature of 235 °C.

Author Contributions: Conceptualization, L.M. and H.Z.; methodology, H.Z. and L.M.; software, H.Z., H.K. and E.V.; validation, L.M., H.Z. and H.K.; formal analysis, H.Z. and E.V.; investigation, H.Z., E.V. and H.K.; resources, H.Z. and L.M.; data curation, H.Z.; writing—original draft preparation, H.Z. and L.M.; writing—review and editing, H.Z. and L.M.; visualization, H.Z.; supervision, H.Z. and L.M. All authors have read and agreed to the published version of the manuscript.

Funding: We are thankful to the Institute of Solid State Physics, University of Latvia, as the Centre of Excellence has received funding from the European Union's Horizon 2020 Framework Programme H2020-WIDESPREAD-01-2016-2017-TeamingPhase2 under grant agreement No. 739508, project CAMART^2. The support of the Strategic Program Excellence Initiative at the Jagiellonian University SciMat (Grant No. U1U/P05/NO/01.05) is gratefully acknowledged by H. Khaksar. This article is partly based upon work from COST Action CA23155, supported by COST (European Cooperation in Science and Technology).

Data Availability Statement: Data are contained within the article.

Acknowledgments: The authors would like to thank Enrico Gnecco from the M. Smoluchowski Institute of Physics, Jagiellonian University for the AFM measurements.

Conflicts of Interest: The authors declare no conflicts of interest.

References

1. Ohtake, N.; Hiratsuka, M.; Kanda, K.; Akasaka, H.; Tsujioka, M.; Hirakuri, K.; Hirata, A.; Ohana, T.; Inaba, H.; Kano, M.; et al. Properties and Classification of Diamond-Like Carbon Films. *Materials* **2021**, *14*, 315. [CrossRef] [PubMed]
2. Leonard, R.L.; Hasan, S.A.; Terekhov, A.Y.; Thompson, C.; Erck, R.A.; Dickerson, J.H.; Johnson, J.A. Protective Coatings for Enhanced Performance in Biomedical Applications. *Surf. Eng.* **2012**, *28*, 473–479. [CrossRef]
3. Zhang, M.; Xie, T.; Qian, X.; Zhu, Y.; Liu, X. Mechanical Properties and Biocompatibility of Ti-Doped Diamond-like Carbon Films. *ACS Omega* **2020**, *5*, 22772–22777. [CrossRef] [PubMed]
4. Liu, J.; Yang, T.; Cao, H.; Deng, Q.; Pan, C.; Wen, F. Diamond-like Carbon Films for Tribological Modification of Rubber. *Nanotechnol. Rev.* **2022**, *11*, 2839–2856. [CrossRef]
5. Gayathri, S.; Kumar, N.; Krishnan, R.; Ravindran, T.R.; Amirthapandian, S.; Dash, S.; Tyagi, A.K.; Sridharan, M. Influence of Transition Metal Doping on the Tribological Properties of Pulsed Laser Deposited DLC Films. *Ceram. Int.* **2015**, *41*, 1797–1805. [CrossRef]
6. Swiatek, L.; Olejnik, A.; Grabarczyk, J.; Jedrzejczak, A.; Sobczyk-Guzenda, A.; Kaminska, M.; Jakubowski, W.; Szymanski, W.; Bociaga, D. Multi-Doped Diamond like-Carbon Coatings (DLC-Si/Ag) for Biomedical Applications Fabricated Using the Modified Chemical Vapour Deposition Method. *Diam. Relat. Mater.* **2016**, *67*, 54–62. [CrossRef]
7. Zhairabany, H.; Dovydaitis, V.; Khaksar, H.; Vanags, E.; Gnecco, E.; Marcinauskas, L. Influence of Molybdenum Concentration on the Microstructure and Nanotribological Properties of Diamond-like Carbon Films. *J. Mater. Sci.* **2023**, *58*, 13437–13448. [CrossRef]
8. Su, Y.; Gong, X.; Huang, W.; Zhang, T.; Hu, R.; Zhang, P.; Ruan, H.; Ma, Y. Enhancing the Tribological Property of Mo-Doped DLC Films in Methanol Using Appropriate Bias Voltage. *Diam. Relat. Mater.* **2023**, *135*, 109795. [CrossRef]
9. Constantinou, M.; Pervolaraki, M.; Koutsokeras, L.; Prouskas, C.; Patsalas, P.; Kelires, P.; Giapintzakis, J.; Constantinides, G. Enhancing the Nanoscratch Resistance of Pulsed Laser Deposited DLC Films through Molybdenum-Doping. *Surf. Coat. Technol.* **2017**, *330*, 185–195. [CrossRef]
10. Sun, H.; Yang, L.; Wu, H.; Zhao, L. Effects of Element Doping on the Structure and Properties of Diamond-like Carbon Films: A Review. *Lubricants* **2023**, *11*, 186. [CrossRef]
11. Zhu, S.; Qiao, Z. Tribology International High Temperature Solid-Lubricating Materials: A Review. *Tribiology Int.* **2019**, *133*, 206–223. [CrossRef]
12. Bahce, E.; Cakir, N. Tribological Investigation of Multilayer CrN/CrCN/TaN Films Deposited by Close Field Unbalanced Magnettron Sputtering. *Rev. Adv. Mater. Sci.* **2019**, *58*, 271–279. [CrossRef]
13. Zeng, Q.; Ning, Z. High-Temperature Tribological Properties of Diamond-like Carbon Films: A Review. *Rev. Adv. Mater. Sci.* **2021**, *60*, 276–292. [CrossRef]
14. Ghadai, R.K.; Shanmugasundar, G.; Vanitha, M.; Čep, R.; Das, S.; Swain, B.P. Investigation of Mechanical Properties of Silver-Doped Diamond-like Carbon Coating by Varying Deposition Temperature. *Front. Mech. Eng.* **2024**, *10*, 1354903. [CrossRef]
15. Chen, Y.; Li, H.; Su, F.; Ma, G.; Li, Q.; Sun, J.; Lin, S. Friction and Wear Behavior of Molybdenum-Disulfide Doped Hydrogen-Free Diamond-like Carbon Films Sliding against Al2O3 Balls at Elevated Temperature. *Wear* **2024**, *544–545*, 205296. [CrossRef]
16. Huang, B.; Liu, L.; Han, S.; Du, H.; Zhou, Q.; Zhang, E. Effect of Deposition Temperature on the Microstructure and Tribological Properties of Si-DLC Coatings Prepared by PECVD. *Diam. Relat. Mater.* **2022**, *129*, 109345. [CrossRef]
17. Dovydaitis, V.; Marcinauskas, L.; Ayala, P.; Gnecco, E.; Chimborazo, J.; Zhairabany, H.; Zabels, R. The Influence of Cr and Ni Doping on the Microstructure of Oxygen Containing Diamond-like Carbon Films. *Vacuum* **2021**, *191*, 110351. [CrossRef]
18. Nečas, D.; Klapetek, P. Gwyddion: An Open-Source Software for SPM Data Analysis. *Open Phys.* **2012**, *10*, 181–188. [CrossRef]
19. Gwyddion, Statistical Analysis Chapter 4. Data Processing and Analysis. Available online: http://gwyddion.net/documentation/user-guide-en/statistical-analysis.html#stat-quantities (accessed on 1 October 2024).
20. Available online: https://www.nanosurf.com/en/products/driveafm (accessed on 1 October 2024).
21. Available online: https://www.nanoandmore.com/AFM-Probe-PPP-LFMR (accessed on 1 October 2024).
22. Bhushan, B. Nanotribology, Nanomechanics and Materials Characterization. In *Springer Handbook of Nanotechnology*; Springer: Berlin/Heidelberg, Germany, 2007; pp. 988–989. [CrossRef]

23. Qiang, L.; Gao, K.; Zhang, L.; Wang, J.; Zhang, B.; Zhang, J. Further Improving the Mechanical and Tribological Properties of Low Content Ti-Doped DLC Film by W Incorporating. *Appl. Surf. Sci.* **2015**, *353*, 522–529. [CrossRef]
24. Zhang, H.S.; Endrino, J.L.; Anders, A. Comparative Surface and Nano-Tribological Characteristics of Nanocomposite Diamond-like Carbon Thin Films Doped by Silver. *Appl. Surf. Sci.* **2008**, *255*, 2551–2556. [CrossRef]
25. Yadav, V.S.; Sahu, D.K.; Singh, M.R.; Kumar, K. Study of Raman Spectra of Nano-Crystalline Diamond Like Carbon (DLC) Films Composition (Sp 2:Sp 3) with Substrate Temperature. In Proceedings of the World Congress on Engineering and Computer Science, San Francisco, CA, USA, 20–22 October 2009.
26. Tang, X.S.; Wang, H.J.; Feng, L.; Shao, L.X.; Zou, C.W. Mo Doped DLC Nanocomposite Coatings with Improved Mechanical and Blood Compatibility Properties. *Appl. Surf. Sci.* **2014**, *311*, 758–762. [CrossRef]
27. Marcinauskas, L.; Šilinskas, M.; Grigonis, A. Influence of Standoff Distance on the Structure and Properties of Carbon Coatings Deposited by Atmospheric Plasma Jet. *Appl. Surf. Sci.* **2011**, *257*, 2694–2699. [CrossRef]
28. Li, H.; Guo, P.; Zhang, D.; Chen, R.; Zuo, X.; Ke, P.; Saito, H.; Wang, A. Influence of Deposition Temperature on the Structure, Optical and Electrical Properties of a-C Films by DCMS. *Appl. Surf. Sci.* **2020**, *503*, 144310. [CrossRef]
29. Wang, Y.; Yin, Z.; Fan, D.; Bai, L. Friction Behaviors of DLC Films in an Oxygen Environment: An Atomistic Understanding from ReaxFF Simulations. *Tribol. Int.* **2022**, *168*, 107448. [CrossRef]
30. Tomala, A.; Pauschitz, A.; Roy, M. Nanotribology of Pulsed Direct Current Magnetron Sputtered Diamond like Carbon Films. *Surf. Sci.* **2013**, *616*, 60–70. [CrossRef]
31. Zhang, S.; Bui, X.L.; Jiang, J.; Li, X. Microstructure and Tribological Properties of Magnetron Sputtered Nc-TiC/a-C Nanocomposite. *Surf. Coat. Technol.* **2005**, *198*, 206–211. [CrossRef]
32. Pei, Y.T.; Chen, C.Q.; Shaha, K.P.; de Hosson, J.T.M.; Bradley, J.W.; Voronin, S.A.; Čada, M. Microstructural Control of TiC/a-C Nanocomposite Coatings with Pulsed Magnetron Sputtering. *Acta Mater.* **2008**, *56*, 696–709. [CrossRef]
33. Zhao, D.; Mei, H.; Ding, J.C.; Cheng, Y.; Zhang, L.; Zhang, T.F.; Kwang, H.K.; Zheng, J. Microstructure and Properties of Mo Doped DLC Nanocomposite Films Deposited by a Hybrid Sputtering System. *Vacuum* **2023**, *208*, 111732. [CrossRef]
34. Su, Y.; Huang, W.; Wang, J.; Gong, X.; Zhang, T.; Hu, R.; Yu, W.; Ruan, H.; Ma, Y. Binary Elements (Si, Mo) Co-Doping Strategy Enhanced the Tribological Performance of Diamond-like Carbon Films. *Surf. Coat. Technol.* **2023**, *471*, 129905. [CrossRef]
35. Kant Tripathi, R.; Singh Panwar, O.; Chockalingam, S. Nanoindentation Study on Nitrogenated Tetrahedral Amorphous Carbon Thin Films with Ultra Low Load. *Indian J. Pure Appl. Phys. (IJPAP)* **2016**, *54*, 543–550.
36. Charitidis, C.A. Nanomechanical and Nanotribological Properties of Carbon-Based Thin Films: A Review. *Int. J. Refract. Met. Hard Mater.* **2010**, *28*, 51–70. [CrossRef]